Transformation of Polyethylene Crystals by High-Pressure Annealing

T. Kazmierczak, A. Galeski

Centre of Molecular and Macromolecular Studies, Polish Academy of Sciences, Sienkiewicza 112, 90–363 Lodz, Poland

Received 25 April 2001; accepted 7 February 2002

ABSTRACT: We investigated the possibility of obtaining high-density polyethylene (PE) samples with crystals in a broad range of thicknesses. PE samples solidified by slow cooling were subjected to hydrostatic pressure at room temperature and then heated to the region of mobile pseudohexagonal form, without being passed through melting. The chains were allowed to rearrange for a period of time to a more extended chain conformation, forming larger crystals. During cooling under pressure, the transformation to orthorhombic crystals of larger thickness occurred. The thickness of the crystals was then controlled by pressure, temperature, and annealing time at high temperatures. The temperature and the pressure in the high-pressure cell was maintained at constant level within 230–295°C and 260–630 MPa, respectively. In this way, we transformed under pressure chain-folded PE crystals to partly chain-extended crystals with peak melting temperatures up to 144.85°C. A range of samples with crystals 20–160 nm thick were produced and characterized with several techniques, including wide- and small-angle X-ray scattering, conventional and temperature-modulated differential scanning calorimetry, dynamic mechanical analysis, and scanning electron, atomic force, and light microscopy as well as low-frequency Raman spectroscopy. Changes in crystallographic unit cell dimensions were observed for crystals with different thicknesses. Crystallinity degree increased with increases in the lamellar thickness up to some level. The initial spherulitic structure deteriorated due to a multifold increase in the lamellar thickness. Oriented samples subjected to annealing in the pseudohexagonal region did not lose the crystal orientation while crystals grew thicker and the crystallinity degree increased; however, no drastic change to noncrystalline phase topology and structure was noticed. © 2002 Wiley Periodicals, Inc. J Appl Polym Sci 86: 1337–1350, 2002

Key words: polyethylene (PE); orientation

INTRODUCTION

The goal of this work was to produce a series of well-characterized polyethylene (PE) samples with crystals in a broad range of thicknesses, from the usual 10–20 nm to chain extended. Such samples are needed for careful and detailed studies of the plastic deformation of crystalline polymers. In the past, the effort to learn as much as possible about the mechanisms of plastic deformation has led to several concepts, including crystal plasticity. However, the real mechanism of polymer crystal plasticity is still not fully comprehended. There are doubts as to whether the crystal plasticity has a mobile dislocation origin (as in low-molecular materials)[1,2] or if it is a partial melting and recrystallization mechanism.[3] It is interesting to learn how the critical shear stresses for certain slip systems depend on crystal stem length and temperature and to compare the results to the prediction of models. This problem was studied recently by Brooks and colleagues[4,5] in a range of crystal thicknesses limited to 10–35 nm. In the past, Popli and Mandelkern[6], on the basis of a similar investigation of yield stress dependence on crystal thickness, concluded that partial melting–recrystallization processes play an important role in the plastic deformation of crystalline polymers. Another problem is the yield-stress dependence on the polymer crystallinity degree, which is not well understood. That is because some of the experimental results have been in contradiction with the model of a semicrystalline polymer. Finally, noncrystalline regions play a significant role in the deformation of semicrystalline polymers. Tie molecules, which link elements in the crystalline phase and take a leading part in the stress transfer, are limited by chain folding. Polymer crystals are subjected to shear stresses via tie molecules, whereas the planes containing chain folds may obscure the slips in crystals. All these problems need to be resolved to know the real mechanisms of polymer crystal plasticity. For this purpose, a series of well-defined mechanical experiments are needed on samples with very well-defined crystalline phases and on crystals of various sizes, in a wide range of thicknesses with narrow distribution and controlled crystal perfection. The knowledge about crystal orientation in the sample would be very useful. Besides, the noncrystalline regions need to be controlled and well characterized.

Correspondence to: A. Galeski (andgal@bilbo.cbmm.lodz.pl).

Contract grant sponsor: Poland State Agency for Scientific Research; contract grant number: 7 T08E 036 19.

The goal of this work was to produce PE samples with crystals in a broad range of thicknesses, from the usual 10–20 nm to chain extended. The other target was to characterize their morphology and crystal structure. The method we used to obtain desirable samples was based on the existence of the region of the pseudohexagonal phase on the phase diagram of PE, in which the formation of significantly thicker crystals is possible. The first observation by Wunderlich and Arakawa[7] indicated that in PE, a pressure above 300 MPa is needed to obtain thick crystals. Crystals as thick as 3 μm were obtained by Geil et al.,[8] which indicates that more than a single extended chain was incorporated within the crystal thickness. Bassett and Turner[9] introduced the term *chain-extended crystals* for the description of such thick crystals obtained under high pressure. As it has been reported by many authors (e.g., refs. 10,11) the crystallinity degree of PE samples crystallized under pressure can reach 99%, and crystal thickness can exceed the length of fully extended polymer chains. It was shown[12,13,14] that under such conditions, the shortest chains are really fully extended, but full extension of longer chains are the exception rather than the rule. The temperature dependence of crystal thickness is similar to chain-folded crystals. Further studies[15] have revealed that the chain-extended crystals are, in fact, large-scale copies of chain-folded crystals. The thickness of PE crystals increases with the increases in the molecular weight (within the range 20–50 kg/mol)[16], increases in pressure at a constant undercooling,[16,17] and increases in crystallization temperature at a constant pressure.[16] It has also been shown that chain-extended crystals can be formed during annealing of chain-folded crystals close to melting temperature.[12,18] Orthorhombic PE crystals are transformed at pressures above 300 MPa to a pseudohexagonal form,[19] and their thickness increases,[20] even to 40 μm.[21] PE samples with a high crystallinity degree in the form of highly chain extended crystals are brittle; the fracture occurs before the yield is reached. However, it seems possible to obtain PE samples exhibiting yielding and differing in crystal thickness and crystallinity.

The purpose of this work was to manipulate the parameters of the crystallization process, the temperature and the pressure, in such a way that samples with crystals of varying thicknesses and varying degrees of crystallinity were obtained. Another question to resolve was if it was possible to produce samples with crystals of various sizes that were preferentially oriented by means of this method.

EXPERIMENTAL

Materials

Two kinds of high-density PE were used in this study: Lupolen 5280HX BASF (Ludwigshafen, Germany); weight-average molecular weight (M_w) = 120,000, M_w/number-average molecular weight (M_n) = 3.4, density = 0.952 g/cm^3 in pellets, melt flow index [MFI; ASTM standard D1238-95] = 2.3 at 190°C/2.16 kg) and Petrothene LS 606-00 Millenium Petrochemicals (Cincinnati, OH); (M_w = 55,000, M_w/M_N = 4.80, MFI = 8.6 at 190°C/2.16 kg, density = 0.960 g/cm^3 in pellets). Additional stabilizers and antioxidants (a mixture of 0.1 wt % IRGANOX1010 and 0.2 wt % IRGAFOS168) were added to prevent excessive oxidation of PE during processing and crystallization.

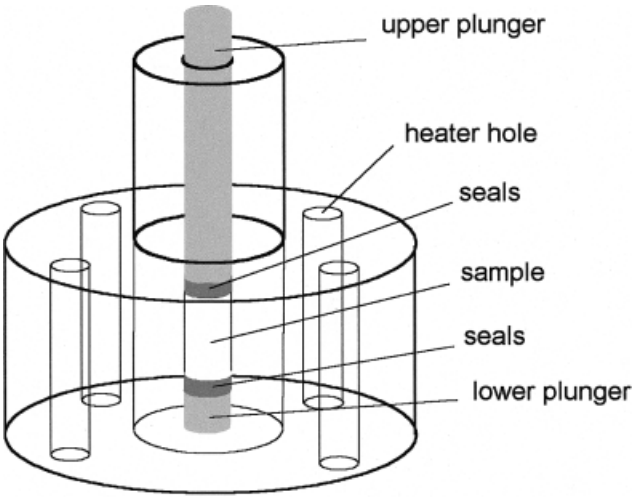

Figure 1 Scheme of the high-pressure cell.

Sample preparation

The samples, in the form of rods, 9.5 mm in diameter, were extruded at a temperature of 160°C from the cylinder of the MFI apparatus into an empty steel cylinder. Such rods were then loaded into a custom-made pressure cell in which the melt-annealing and crystallization processes under high pressure were conducted. The cell, shown in Figure 1, was made of ultra high-strength steel (30HGSNA type) capable of applying pressure up to 1000 MPa at the temperature up to 320°C. A cylindrical channel was drilled along the axis of the cell, with very high surface smoothness (roughness in the range of 0.02–0.12 μm) and high diameter accuracy (maximum deviation = 0.4–0.6 μm). Tungsten carbide rods (hardness = 46–47 HRc, which corresponds to a hydrostatic pressure within the cylinder of 1650–1680 MPa), tightly matching the diameter and smoothness of the cylindrical opening in the cell, were used as plungers. The high accuracy of fitting of the punches to the channel and additional brass sealing prevented the highly compressed polymer from any leakage out of the cell. Four electrical heaters (600 W total power) were controlled by a temperature controller, which ensured a temperature accuracy of 1°C inside the cell. The temperature sensor

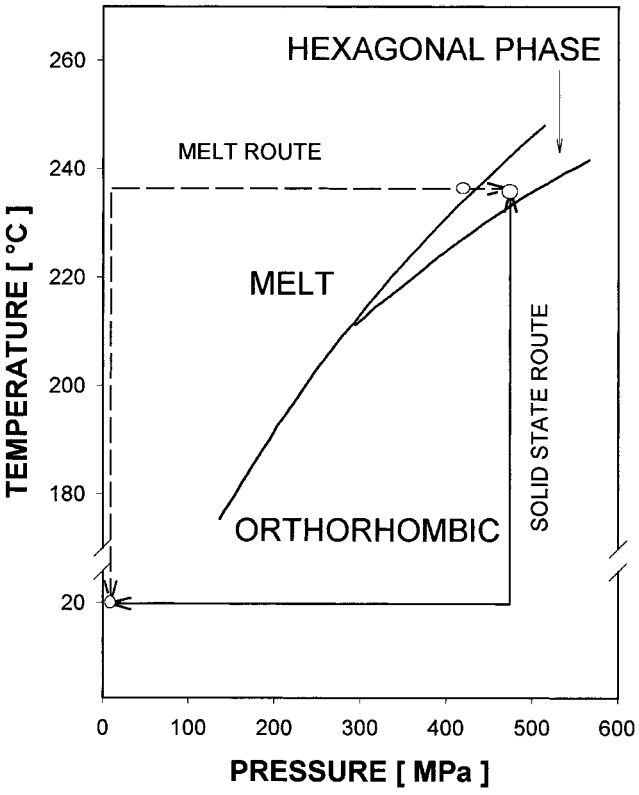

Figure 2 Exemplary phase diagram for PE. The crystal transformation route employed in the studies is shown. The points indicate the conditions for the samples chosen for the detailed studies.

was placed 10 mm away from the sample in a narrow 1-mm thick channel, perpendicular to the wall of the cell. The polymer was compressed by the use of an Instron tensile testing machine (Instron Corp., High Wycomb, UK), via a fixture that stabilized the load exactly along the cell axis. The hydrostatic pressure inside the cell was controlled by means of a tensile testing machine with an accuracy of ± 0.5 MPa.

The high-pressure transformation of samples was performed by annealing at an elevated temperature under high pressure. In most cases, the samples placed inside the pressure cell were subjected to high hydrostatic pressure at room temperature and only then heated up to the defined temperature. Such a procedure is contrary to the usual method, where samples are melted and then the pressure is applied. After annealing, the samples were cooled to room temperature, and then the pressure was released. The routes of the sample in pressure and temperature ranges are shown schematically in Figure 2. The experiments included annealing in a wide range of temperatures and pressures around the region of the pseudohexagonal packing of PE, from 230 to 295°C and from 260 to 630 MPa. In some experiments, the transformation to pseudohexagonal phase took place in the course of cooling to room temperature when the sample was annealed in molten state, whereas in others, the transformation occurred during annealing. In the first case, the time of annealing was of no importance, whereas the rate of cooling through the pseudohexagonal zone defined the obtained structure. In the second case, the time of annealing within the pseudohexagonal region defined the obtained crystal sizes and morphology.

In some other cases, the samples were first heated and then pressurized to obtain samples with thicker crystals.

Differencial scanning calorimetry (DSC)

The thermal analysis of the samples was conducted with a TA2100 DSC apparatus (TA Instr., New Castle, DE) which was indium calibrated. Small pieces, with a total mass of 6 mg, were cut from the core of rods, placed into aluminum pans, and pressed slightly to ensure good thermal contact with the DSC cell surface. The melting thermograms were recorded at a heating rate of 10°C/min, under a nitrogen flow. The crystallinity level and lamellar thickness (l^*) were estimated on the basis of the heat of melting of the sample recorded during heating from 60 to 160°C and from the recorded melting temperature (T_m), respectively. For the determination of lamellar thickness, the following equation was used:[22]

$$l^* = \frac{2\sigma_e T_m^0}{\Delta h_f (T_m^0 - T_m)} \tag{1}$$

where σ_e is the lamellar basal-surface free energy (for PE, $\sigma_e = 9 \times 10^{-6}$ J/cm^2),[23] h_f is the heat of fusion per unit volume (for PE, $h_f = 293$ J/cm^3),[24] and T_m^0 is the extrapolated equilibrium T_m measured for PEs, used in this work at 145.1°C, as measured earlier by us for Petrothene LS 606-00 PE.[25]

Temperature-modulated differencial scanning calorimetry (TMDSC)

Modulated DSC is a technique that also measures the difference in heat flow between a sample and an inert reference as a function of time and temperature. In addition, the same heat flux cell design is used. However, in TMDSC, a different heating profile (temperature regime) is applied to the sample and reference. Specifically, a sinusoidal modulation (oscillation) is overlaid on the conventional linear heating or cooling ramp to yield a profile in which the average sample temperature continuously changes with time but not in a linear fashion. The total heat flow, which is the only heat flow measured by conventional DSC, is composed of two components:[26]

$$dQ/dt = C_p\beta + f(T,t) \quad (2)$$

where dQ/dt is the total heat flow, C_p is the heat capacity, β is the heating rate, and $f(T,t)$ is the heat flow from kinetic (absolute temperature and time-dependent) processes. One component is a function of the sample's heat capacity and the rate of temperature change, whereas the other is a function of absolute temperature and time. TMDSC determines the total, as well as these two individual heat flow components, to provide increased understanding of complex transitions in materials. TMDSC is able to do this on the basis of the two heating rates seen by the material: the average heating rate, which provides total heat flow information, and the sinusoidal momentary heating rate, which provides heat capacity information from the heat flow that responds to the rate of temperature change.

These individual heat flow components are often referred to by different names: the heat capacity component and reversing heat flow.

A temperature-modulated differential scanning calorimeter TA 2920 from TA Instruments was used in this study. The heating in the calorimeter was performed with a constant heating rate of 1°C/min, on which the sinusoidal temperature oscillation was superimposed with a temperature amplitude of 0.159°C and a period of temperature oscillation of 60 s. These parameters were selected in such a way that the instantaneous heating rate varied between some positive value and zero (isothermal). These parameters defined the "heating only" mode, for which the minimum momentary heating rate was 0°C/min. The period of oscillations was set long enough to achieve at least four modulations at half-height of the melting peak.

Atomic force microscopy (AFM) and scanning electron microscopy (SEM)

The morphological features of the samples were investigated by means of an atomic force microscope constructed in the Physics Department of the University of Lodz in Poland. The samples were cut from the core of the samples, and their surfaces were microtomed with a freshly prepared glass knife. We then treated the surfaces by permanganic etchant[27] to reveal lamellar details in PE. We prepared reagents by dissolving 0.7 wt % potassium permanganate in a mixture of two parts by volume concentrated sulphuric acid (98%) and one part ortho-phosphoric acid (85%). The etching was conducted at 18°C for 4.5 h. Then, the samples were carefully washed with a procedure described elsewhere.[27] The AFM scans were performed in air, with a Si_3N_4 tip. The height and deflection mode images were recorded simultaneously.

Samples prepared in the same way were used for the study of morphology by means of SEM. A JEOL 5500LV scanning electron microscope (Jeol Ltd., Akishima, Tokyo) was used at an accelerating voltage of 10 kV. Prior to microscopy examination, the surfaces of the samples were covered with a thin layer of gold by ion sputtering.

Wide-angle X-ray scattering (WAXS)

The orientation of the crystalline phase of high-density PE was studied by means of X-ray diffraction with pole figures. A WAXS system consisting of a computer-controlled pole figure device associated with a wide-angle goniometer coupled to a sealed tube X-ray generator operating at 30 kV and 30 mA was used in this study. The X-ray beam consisted of CuKα radiation filtered by a Ni filter and electronically. For pole figure data acquisition and construction, we used a procedure elaborated earlier.[28] The complete pole figures were obtained for the projections of Euler angles of the sample orientation with respect to the incident beam, including the diffraction in reflection and transmission modes.

Small-angle X-ray scattering (SAXS)

SAXS was used for the study of lamellar structure. A PW 1830 generator Philips Analytical X-ray B.V., Eindhoven, The Netherlands) operating at 50 kV and 30 mA (CuKα radiation, filtered by a Ni filter) and a Kiessig-type pinhole camera equipped with a collimator system providing point illumination were used. The distance between the sample and the detector was settled at 1100 mm. The exposition time was 20 h. The beam divergence and the incident beam stopper of the camera allowed for resolution of the scattering structures up to 80 nm in thickness. The two-dimensional SAXS patterns were recorded on imaging plates (Kodak) in vacuum conditions. Exposed imaging plates were read with a PhosphorImager Si scanner (Molecular Dynamics, Sunnyvale, CA). The values of the long period (L) were evaluated on the basis of the scattered intensity patterns with the Bragg formula:

$$L = \frac{\lambda}{2 \sin \theta_{max}} \quad (3)$$

where λ is the X-ray wavelength ($\lambda_{CuK\alpha}$ = 0.15 nm) and θ_{max} is the scattering angle corresponding to the first-order maximum in the SAXS pattern.

Raman spectroscopy

Low-acoustic-frequency Raman spectra were used for the determination of crystal thickness. The frequency

TABLE I
Set of High-Density PE Lupolen 5280HX Samples with Crystals of Various Sizes

Sample	Crystallization route	Temperature (°C)	Pressure (MPa)	Time (min)	T_m (°C)	L (nm)	χ (%)
1	Nonannealed	—	—	—	132.25	20	64
2	I	247	260	30	132.65	21	71
3	II	235	400	60	136.50	30	75
4	I	247	630	60	139.95	50	93
5	II	235	430	60	142.25	90	90
6	II	267	630	60	142.80	110	90
7	II	295	630	5	143.50	160	88
8	II	235	480	60	144.85	1030	85

Crystallization and annealing sequence and conditions: (I) heating to annealing temperature, increasing pressure, annealing, cooling, and reducing pressure: (II) increasing pressure, heating, annealing, cooling, and reducing pressure. T_m and crystal thickness (L) as obtained from the Hoffman-Weeks equation [eq. (1)], assuming a constant lamellar basal free energy ($\sigma_e = 9.10^{-6}$ J/cm^2), χ-crystallinity assuming heat of crystal melting $\Delta h_f = 293$ J/g are depicted.[24]

shift of a low acoustic peak with respect to the frequency of the excitation light ($\Delta\nu$ expressed in cm^{-1}) depends on the length of vibrating chain (L) and on the velocity of sound along the chain [expressed by $(E/\rho)^{-1/2}$ where E is Young's modulus and ρ is the density of crystals] in the following way:[29]

$$\Delta\nu = (m/2Lc)(E/\rho)^{1/2} \quad (4)$$

where m is the order of the vibrational mode and c is the velocity of light. The previous formula was derived first for paraffin crystals[29] and later applied to PE.[30–34] When PE crystal density is assumed to be 1 g/cm^3 and the Young's modulus of PE crystals is 360 GPa[34] (this value of Young's modulus was determined by Lemstra et al.[34] with a sample with known vibrating chain length, crystal density, and excitation light frequency, whereas the theoretical value of Young's modulus was equal to 405 GPa as it followed from the consideration of C—C bond extension[35]), the thickness of lamella is calculated on basis of the following formula:

$$L = 316.0/\Delta\nu \quad (5)$$

where L is the thickness of lamella in nm and $\Delta\nu$ in cm^{-1} is the position of the peak associated with the first-order longitudinal acoustic mode (LAM-1).[36]

Low-acoustic-frequency Raman spectra of crystallized PE samples were recorded by means of a Raman spectrometer Z40 (DILOR, Jobin-Yvon SA, Longjumeau Cedex, France) with five diffraction grids. The source of the light was an argon laser ($\lambda = 514.5$ nm) with a power of 120 mW. No special care for better peak resolution was taken. In this way, we were able to locate the low-acoustic-frequency peak with a resolution better than 0.5 cm^{-1}. The largest crystals that could be detected in this way did not exceed 60–65 nm thickness. The information on thickness of lamellar crystals as determined from low-acoustic-frequency Raman spectra differs from that obtained from SAXS in several aspects: first, unlike in SAXS, the existence of a LAM-1 peak in Raman spectra does not mean that the lamellae are arranged in stacks; second, the LAM-1 peak is sensitive to the length of chain span between lamellae basal surfaces; that is, the chain tilt with respect to the basal surfaces of lamellar crystals is not considered in the lamellar thickness determined from Raman spectra. In a more rigorous treatment of low-acoustic Raman spectra, the polydispersity of the length of extended chains, fold surfaces, and branches that result in LAM-1 peak broadening should be considered.

Dynamic mechanical thermal analysis (DMTA)

The dynamical mechanical measurements of the samples were carried out by means of a DMTA MkIII apparatus (Rheometric Scientific, Inc., Epsom, UK) in the single cantilever mode at 1 Hz and a heating rate of 2°C/min. The specimens for DMTA studies in the form of $1 \times 4 \times 12$ mm bars were machined with slow speed from the PE rods.

RESULTS AND DISCUSSION

Using different values of temperature, pressure, and time of annealing, we obtained a series of high-density PE samples that showed a wide range of melting temperatures and various levels of crystallinity. An exemplary set of such samples is presented in Table 1. Crystallization conditions, T_m, and crystal thickness, as obtained from the Hoffman–Weeks equation [eq. (1)], with an assumption of constant lamellar basal free energy ($\sigma_e = 9 \times 10^{-6}$ J/cm^2), are shown. The materials represent a series of high-density PE samples having crystals with average thicknesses in a wide range, from 20 nm up to more than 1000 nm. However, the largest value of crystal thickness was obtained on the basis of eq. (1) when unchanged value of the lamellar basal free energy

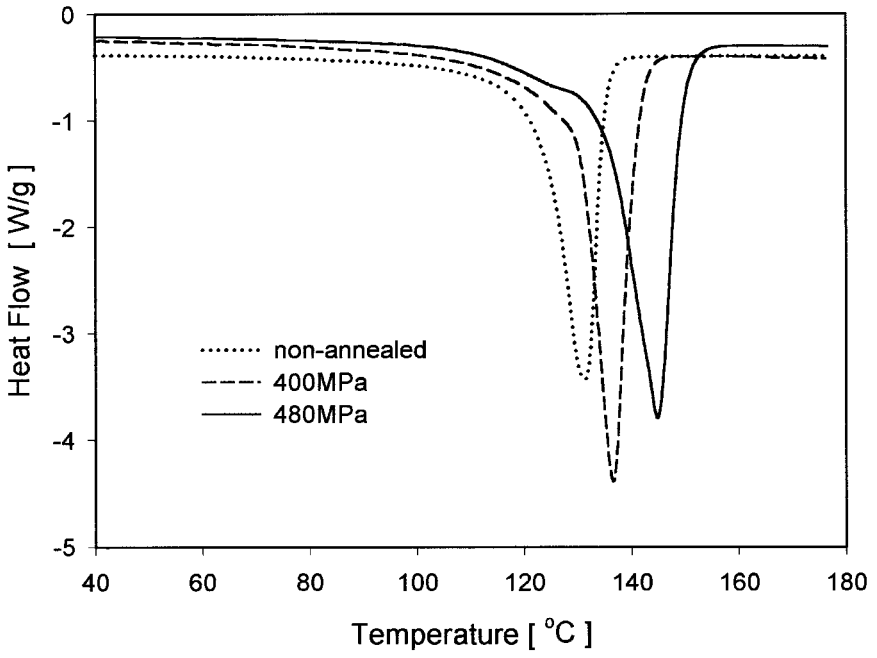

Figure 3 DSC thermograms for high-density PE samples annealed under different conditions.

was assumed, despite the fact that the basal crystal surface was now relatively free from chain folds. Hoffman et al.,[37] while describing the dependence of polymer crystal growth rate on molecular weight, developed a formula describing the free energy in terms of the number of chain folds and cillia. When only folds and chain ends form the lamellar basal plane, the value of σ_e is described by the following empirical formula valid for PE:[37]

$$\sigma_e = 93[(f + 0.153)/(f + 1)]\ [\mathrm{erg/cm^2}] \qquad (6)$$

where f is the number of folds per single macromolecule. It follows from eq. (6) that if no folds are incorporated in the lamellar basal plane (f=0), the value of σ_e is equal only to 14.2 erg/cm^2 = 1.42 $\times$ 10^{-6} J/cm^2 instead of 90 erg/cm^2 = 9 $\times$ 10^{-6} J/cm^2, as for usual PE crystals. The lamellar thickness 1030 nm for the sample 8 from Table 1, as obtained from eq. (1), was so large that we could assume that there were nearly no chain folds. It follows then that the true thickness of the lamellae in sample 8 was only 160 nm instead of 1030 nm, as calculated from the DSC data with the assumption σ_e = 90 erg/cm^2. As is evident from the SEM examination, described further in this article, the true thickness of the lamellae in this sample was around 160 nm. That value agreed well with the thickness of lamellae obtained from DSC, when the reduced level of lamellae basal free energy due to zero concentration of chain folds was assumed.

Unfortunately, the corrected values of lamellar thickness for other PE samples from Table 1 could not be calculated because we had no detailed information on the fraction of folds present in their crystals.

In further consideration and examination, we focused on three samples made from the high-density PE Lupolen 5280HX extruded rods: non annealed (sample 1 from Table 1), annealed at 235°C under 400MPa (sample 3 from Table 1), and annealed at the same temperature but under 480MPa (sample 8 from Table 1). In the two last cases, the annealing was maintained for 1 h. The sample under 400MPa was annealed in the molten state, and eventual transformation to thicker crystals occurred during cooling through the pseudohexagonal region, whereas the sample under 480 MPa was annealed within the pseudohexagonal region and did not pass through melting. Figure 3 shows the DSC thermograms for these samples. A significant shift of the melting peak to a higher temperature for annealed samples was caused by the increased thickness of crystals. The crystal thicknesses of these samples, calculated on the basis of eq. (1), were 20 nm for non annealed, 30 nm for annealed under 400 MPa pressure, and 160 nm for annealed samples under 480 MPa pressure when no chain folding was assumed. The last value indicated that the macromolecular chains in the crystals were highly extended, with only two to three folds per chain. The length of fully extended chains of Petrothene LS 606-00 (M_w = 55,000) PE was roughly 500 nm (CH_2—CH_2—CH_2 sequence length in the crystal equal to 0.2547 nm[38]).

The samples differed also in crystallinity (see Table 1).

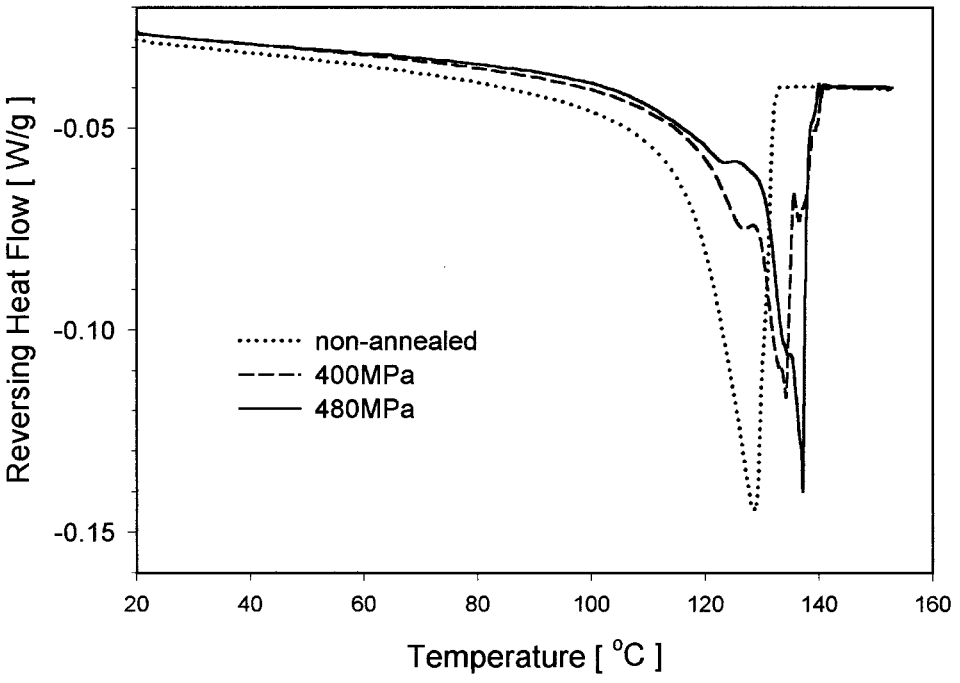

(a)

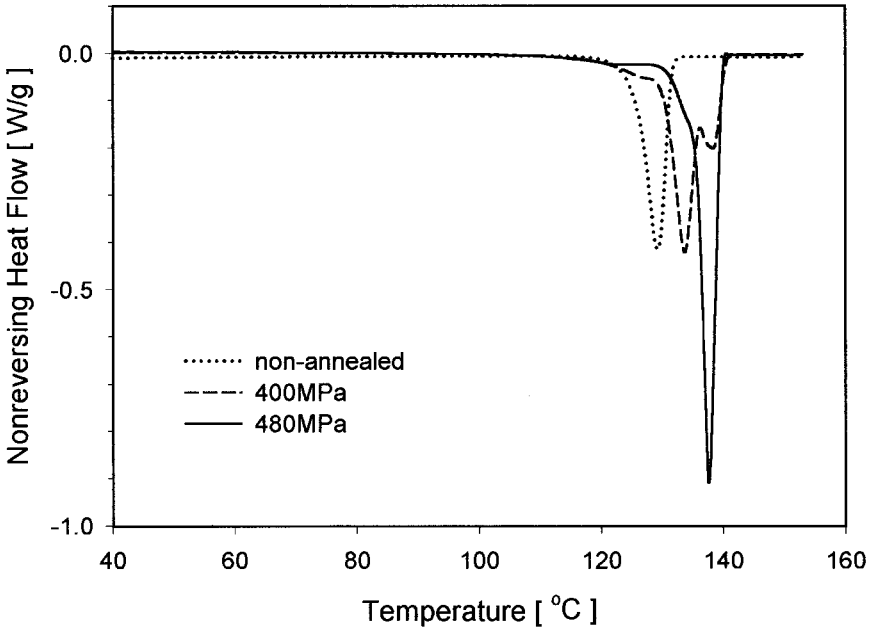

(b)

Figure 4 TMDSC thermograms for high-density PE samples annealed under different conditions: (a) reversing heat flow and (b) nonreversing heat flow.

To obtain more precise information about the structure and morphology of the samples, we performed detailed investigations, employing several techniques.

TMDSC

Thermograms of reversing and nonreversing heat flow recorded during modulated heating with an average rate of 1°C/min are shown in Figure 4(a,b). They reveal the existence of two populations of crystals in the samples annealed under a pressure of 400 MPa. Both populations consisted of crystals a size larger than those in the nonannealed sample, as could be judged from the positions of respective peaks on the nonreversing heat flow curves in Figure 4(b). The area under the lower temperature peak was larger, which

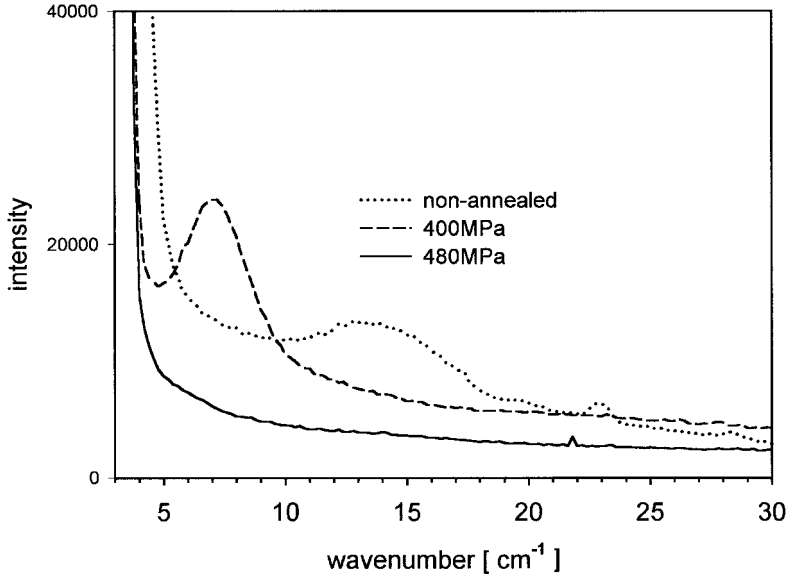

Figure 5 Low-frequency Raman spectra for high-density PE samples annealed under different conditions.

means that the population of smaller crystals was larger. In the case of the sample annealed under 480 MPa, the peak related to smaller crystals disappeared, and most crystals had a large size.

An interesting feature of the annealed samples, which was revealed by both DSC and TMDSC measurements, was that crystals of the smallest size, corresponding to a small shoulder on the conventional DSC thermograms at 129–132°C for annealed samples, were apparently formed during cooling. Crystals in the sample annealed at 400 MPa were certainly formed during cooling because at annealing conditions, the sample was in the molten state. A small fraction of crystals with similar T_m's was formed in the sample annealed at 480 MPa (the pseudohexagonal form region of temperature and pressure). It was apparent that these crystals were also formed during cooling. This last observation indicated that the crystal transformation, which occurred in the pseudohexagonal form region of high temperature and pressure, left small uncrystallized regions between large thick crystals that could be filled with small crystals only at lower temperatures during cooling.

Raman spectroscopy

The low-frequency spectra of the samples studied are shown in Figure 5. For the non annealed sample and the sample annealed under 400 MPa, there was a LAM-1 peak indicating corresponding to the crystal thickness. For the sample annealed under 480 MPa, no peak could be resolved: apparently, the crystal thickness was so large that it was above the resolution power of the Raman apparatus. On the basis of the peak's positions, the lamellar thickness for the nonannealed sample and the annealed sample under a pressure of 400 MPa was at the level of 25 and 46nm, respectively. These values were in good agreement with the estimation on the basis of the DSC data at 20 and 30 nm, respectively (see Table 1).

SAXS

The exemplary SAXS patterns recorded for the nonannealed sample are presented in Figure 6. Similarly to the longitudinal acoustic mode in Raman spectra, the resolution of SAXS is limited to crystals smaller

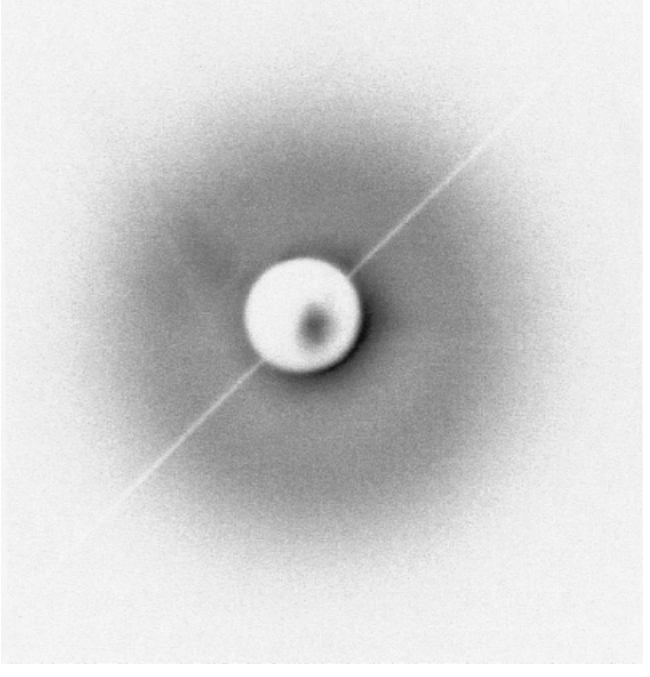

Figure 6 Exemplary SAXS pattern for the nonannealed high-density PE sample.

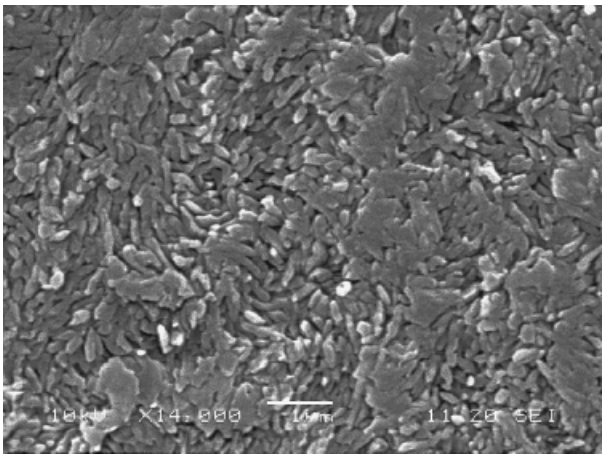

Figure 7 Scanning electron micrograph of the surface, exposed by microtoming and etching, of high-density PE samples annealed at 235°C under 480 MPa.

than approximately 80 nm: the scattering rings could be resolved only for nonannealed samples and samples annealed under 400 MPa. No scattering ring could be resolved for the sample annealed under 480 MPa. The long period, which included the lamellar thickness and the thickness of a corresponding interlamellar material as calculated from the position of the scattering maxima, were 25 nm for the nonannealed sample and 44 nm for the annealed sample under a pressure of 400 MPa. When the crystallinity degree of the samples was considered (Table 1), these values corresponded to 16 and 33 nm crystal thickness for the nonannealed sample and the sample annealed at 400 MPa; respectively. The long period for the sample annealed under a pressure of 480 MPa was above the SAXS apparatus resolution and could not be measured in this way.

Morphology

The SEM and AFM micrographs presented in Figures 7 and 8(a,b), respectively, show lamellar morphology for annealed samples. In the case of samples annealed under a pressure of 480MPa, the lamellae appeared much thicker (about 160 nm) than in the samples annealed under a pressure of 400 MPa. However, lamellae in the sample annealed at 400 MPa seemed to be better developed, and they were relatively longer with respect to their thickness, which was about 30 nm. Some of the lamellae in the sample annealed under 400 MPa seemed to be very well developed in their lateral dimensions, whereas in the sample annealed under 480 MPa, their lengths rarely exceeded three times their thicknesses. Reasons for this followed from different conditions in which the lamellae grew: for the sample that was annealed under 400 MPa in the molten state, the lamellae grew mostly from the melt via a nucleation mechanism because the pseudohexagonal phase was not formed during cooling. The mechanism of growth was probably the same as in a polymer crystallized in ambient conditions. Lamellae in the samples annealed at 480 MPa did not pass through the melt, but they were transformed to a pseudohexagonal form and grew in thickness more than eight times, from an initial 20 nm to 160 nm. Their lateral dimensions seemed unchanged, which indicated that they were produced from the ones that were initially present in the samples forming spherulites.

WAXS

The 2θ difraction scans of Petrothene samples nonannealed and annealed (630 MPa, 257°C, 1 h see the

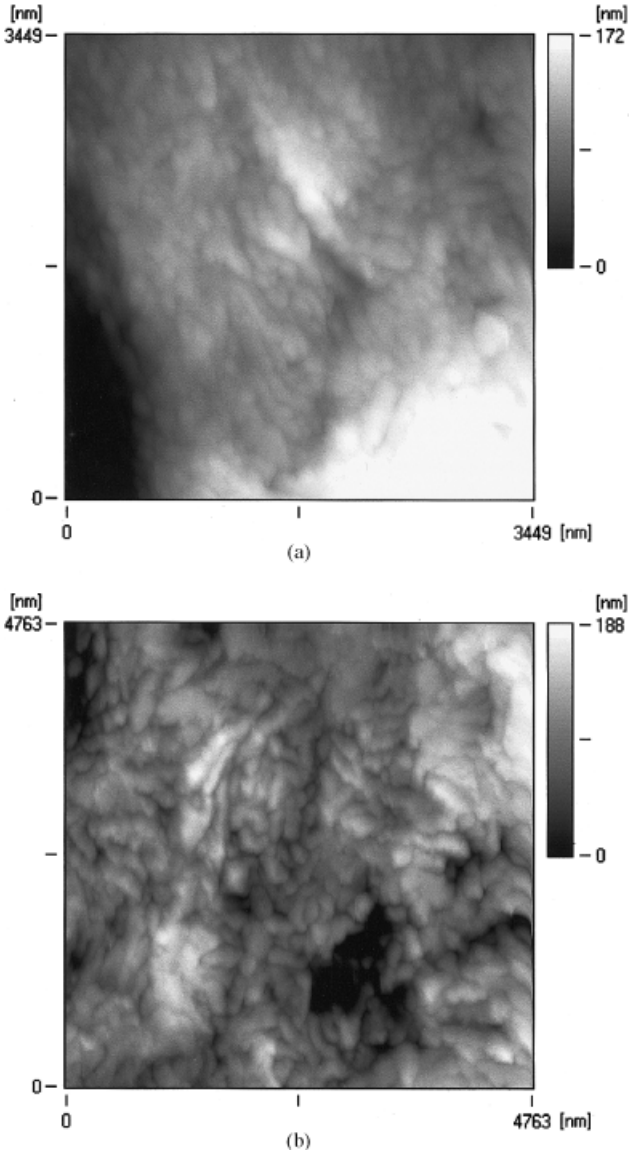

Figure 8 Atomic force micrographs of surfaces, exposed by microtoming and etching, of high-density PE samples annealed at 235°C under different pressures: (a) 400MPa and (b) 480MPa.

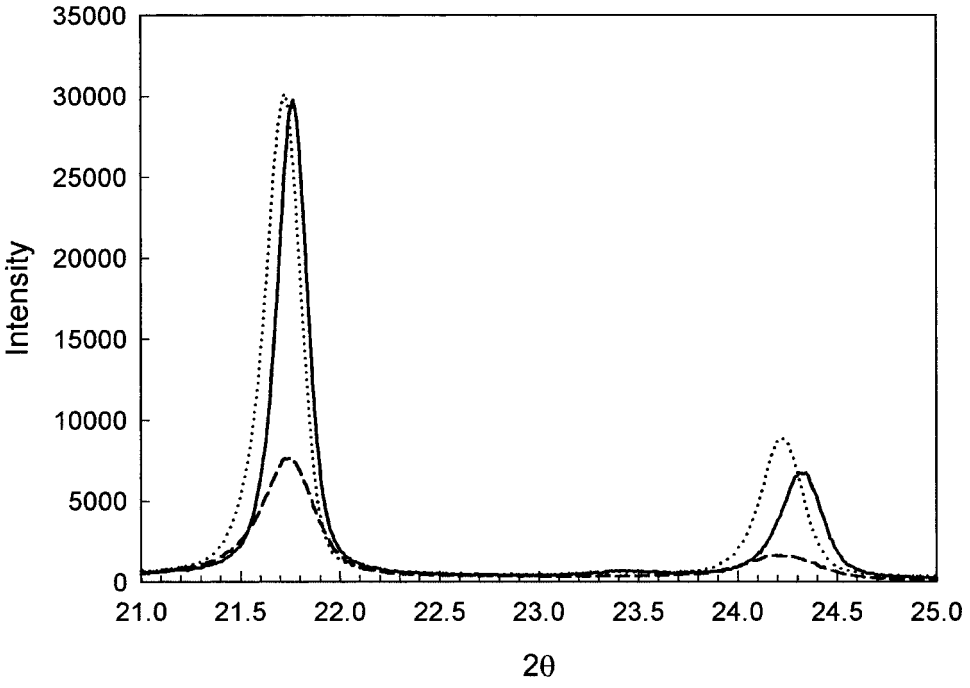

Figure 9 Wide-angle X-ray diffraction 2Θ scans of various PE samples: (---) Petrothene non-annealed (···) Petrothene annealed (630 MPa, 257°C, 1 h), and (—) SNPA Elf-Aquitaine, M_w/M_n = 1.1, annealed (630 MPa, 257°C, 1 h).

procedure described in Table 1 as 1) are presented in Figure 9. For comparison, the 2θ scans for the PE sample with perfect crystals [monodisperse high-density PE, SNPA Elf-Aquitaine, M_w/M_n = 1.1, equilibrium T_m = 145.3°C, while crystallized at 630 MPa and 257°C for 1h (procedure I) with T_m = 144.9°C and crystallinity degree = 91%) is presented. Crystals in the nonannealed sample were not very well developed, and the overall crystallinity was lower than in the annealed sample. The crystal unit cell packing seemed not to be largely different than in the annealed sample; however, the level of crystallinity was much higher in the annealed sample (crystals thickness = 170 nm, crystallinity degree = 92% as it followed from DCS measurement).

Refinement of packing, which manifests by the shift of the peak's position to higher angles, was achieved for PE

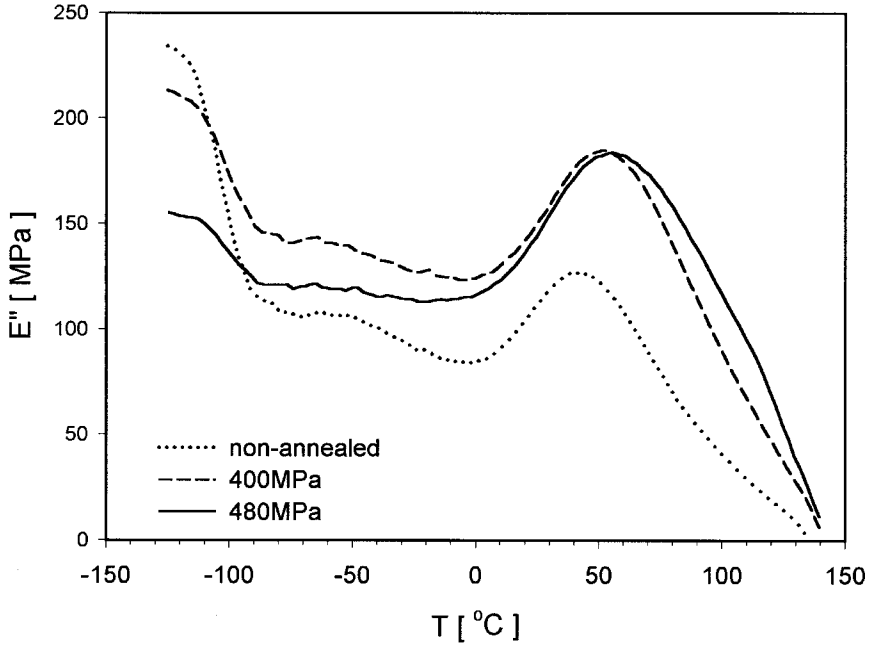

Figure 10 Temperature dependence of E″ of high-pressure PE samples annealed under different conditions.

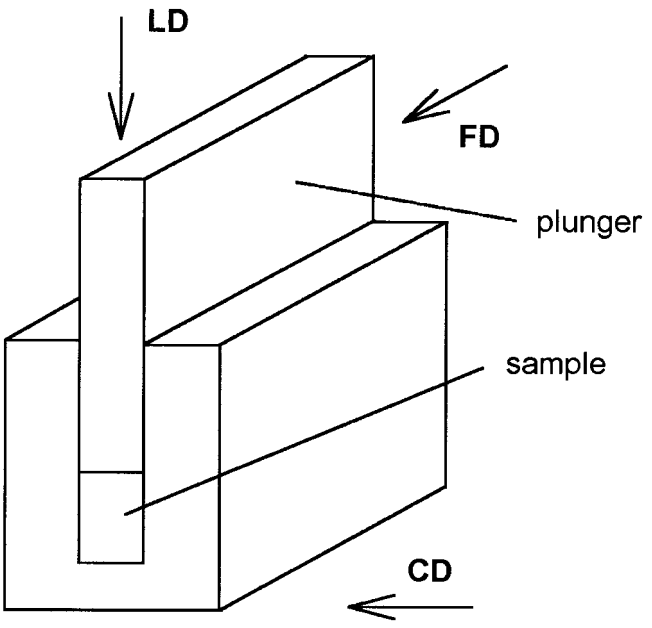

Figure 11 Scheme of a channel die.

with very narrow polydispersity (M_w/M_n = 1.1). This was the result of the very high crystallinity of this sample and the very large crystals (670 nm as it followed from the T_m determined in DSC) grown during annealing at high pressure. Apparently, the perfection of chain-extended crystals depends on the influence of defects caused by chain ends: in PE with very narrow molecular-weight dispersity, there was a little fractionation, and most of the crystals were built from chains of similar length. In such cases, the chain ends were located at the faces of the chain-extended crystal. Also, the crystallinity degree reached a very high level (91 wt % as it followed from the melting heat determined in DSC). With little amorphous phase, the stresses at crystal–amorphous interfaces were low. This last conclusion was supported by the fact that the monodisperse PE sample with chain-extended crystal was very fragile; apparently, chain-extended crystals inside the sample were not very well interconnected and bonded to each other. All these effects resulted in very good crystal packing in the nearly monodisperse PE sample.

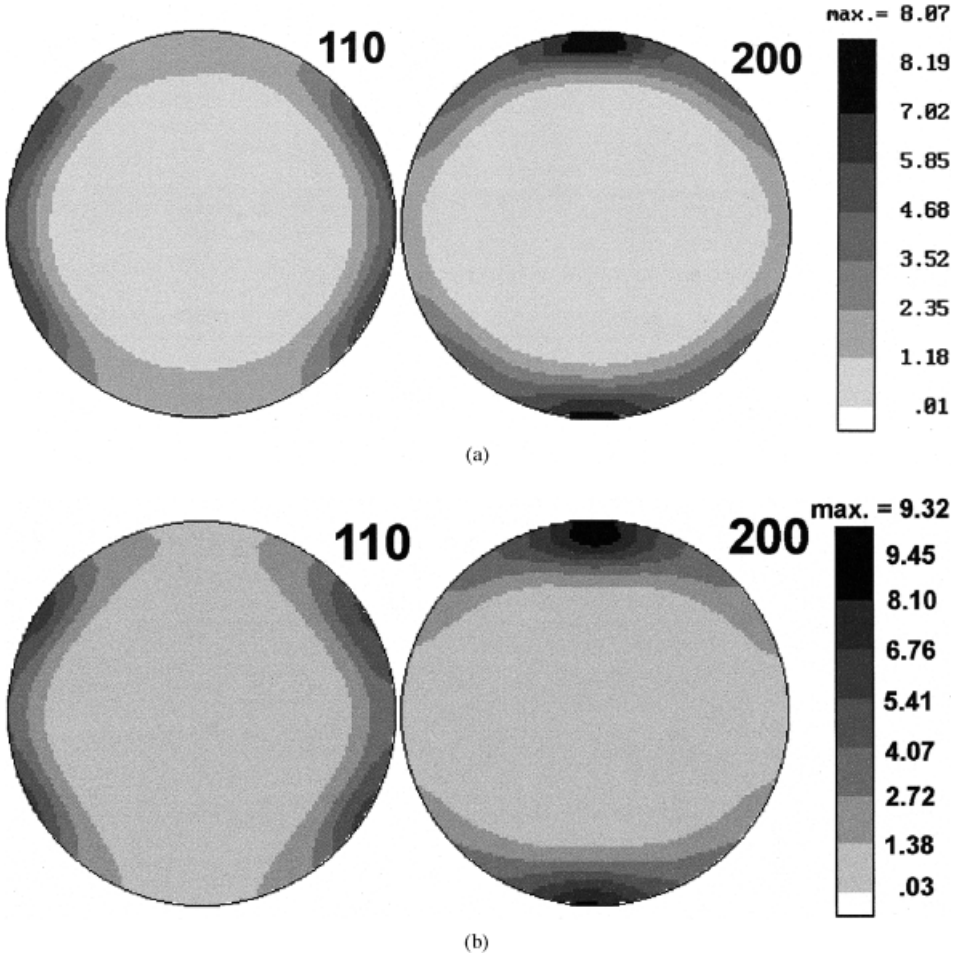

Figure 12 Pole figures of a PE sample (a) deformed in a channel die to the compression ratio of 6 and (b) then subjected to high-pressure transformation at 257°C under a pressure of 630 MPa. The deformed sample showed single crystal texture, which was unchanged after high-pressure transformation.

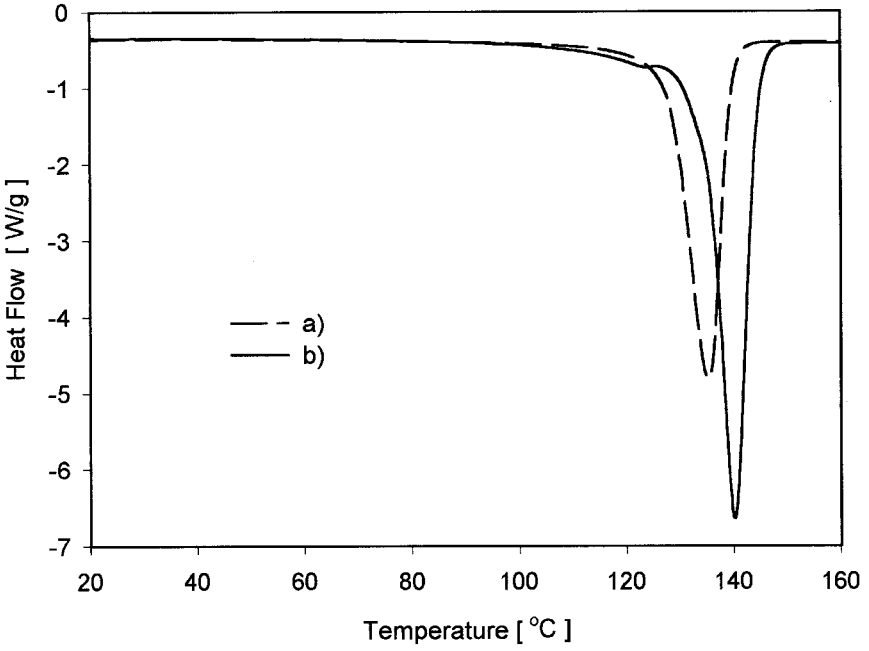

Figure 13 DSC scans of (a) high-density PE sample deformed in a channel die at 130°C to a compression ratio of 6.0 and (b) the same sample after annealing in the pseudohexagonal region at 257°C under a pressure of 630 MPa without passing through the molten state.

DMTA

Dynamic mechanical measurements showed peaks of low-temperature and high-temperature relaxation processes (see Fig. 10). The process at low temperatures, below −100°C, which was associated with the glass transition, showed highest intensity for the sample with the lowest crystallinity, that is, for the nonannealed sample. The difference in intensity for both annealed samples was smaller but agreed well with the difference in the crystallinity level for both samples. The interpretation of the high-temperature process, above 0°C, was more complicated as this process is associated with the relaxation of crystallites.[39,40] Usually the increase in the intensity of this process is connected with a higher content of crystalline phase in the sample.[39,40] In our samples, this process was also more intense for the samples with higher levels of crystallinity. Another interesting feature was the shift of the peak of high temperature process on the dynamic mechanical imaginary modulus (E'') versus temperature plot (see Fig. 10). The positions of the high temperature peak were 39°C for the nonannealed sample, 51°C for the 400 MPa annealed sample, and 55°C for the 480 MPa annealed sample. The shift of the peak position was correlated with the crystal thickness in the samples: 20, 30, and 160 nm, respectively. That is because for larger crystals, the activation energy for their relaxation was higher and a higher temperature was needed to activate the relaxationmovements. Hence, for thicker crystals, the peaks of high-temperature relaxation processes were located at higher temperatures.

X-ray pole figures

We applied the technique of X-ray pole figures to study the orientation behavior of the crystals during the transformation to chain-extended crystals while annealing the sample within the pseudohexagonal form region. Their lateral dimensions seemed unchanged, as it followed from SEM and AFM observations described previously. This was an indication that they were formed by thickening from the ones that were initially present in the sample. To test this possibility, we proposed following experiment: a high-density PE (Petrothene) sample shaped to a plate (10 $\times$ 10 $\times$ 60 mm was deformed in a channel die (Fig. 11) to a compression ratio of about 6.0. The process was performed at a temperature of 130°C with a plunger speed of 0.1 mm/min. Channel die compression resembles plane–strain deformation and produces a well-defined quasi single-crystal texture for PE.[41] The texture of such a sample was determined by WAXS, and the respective pole figures were constructed from X-ray diffraction data for crystallographic (100) and (200) planes of orthorhombic PE crystals. Figure 12(a) presents these pole figures. Darker areas show the clustering of normals to the particular crystallographic planes. Indeed, the pattern presented in Figure 12(a) resembles single-crystal texture. From the deformed sample, a round rod was machined with a size match-

ing the diameter of the high-pressure cell. The prepared rod was placed in the high-pressure cell, pressurized at 630 MPa, heated to 257°C, and then annealed at 257°C under 630 MPa for 1 h, that is, in the pseudohexagonal phase zone without passing through the melt. The sample was cooled to room temperature, and the pressure was released. Then, the texture was again investigated by means of X-ray pole figures. Pole figures for the oriented annealed sample are presented in Figure 12(b). They showed essentially the same strong single-crystal texture as before annealing. It was proven then that the annealing in the pseudohexagonal phase region did not cause the loss of orientation of crystals in the sample. At the same time, the thickness of crystals and the level of crystallinity, as seen from the DSC scan in Figure 13, increased dramatically: from the increase of the temperature of melting peak from 135.3 to 140.14°C, the crystal thickness increased from 28 to 55–60 nm, whereas the crystallinity degree increased from 74% to as high as 98.5%, as judged from the increase of the heat of melting from an initial 217.1 to 288.6 J/g (100% crystalline PE should show the heat of melting of 293 J/g[24]). From the previous observations, it follows that the orientation of those crystals that got thicker was not lost. Simple calculation showed that the number of crystallites in the annealed sample was reduced at least by 30% when it was assumed that they did not grow in lateral directions but only got thicker. If the crystals increased their lateral dimensions, the number of crystals would be more reduced. The material from those crystals that disappeared and the surrounding amorphous material were consumed by thickening crystals in such a way that the crystals grew in thickness, preserving the orientation of the precursor original crystal. No new crystals with a random orientation were formed in the sample in the annealing condition.

Light microscopy

The microtomed slices of the nonannealed and annealed samples are presented in Figures 14(a–c). The initial morphology of the nonannealed sample was a typical spherulitic structure and is presented in Figure 14(a). Spherulites totally filled the volume of the sample and were roughly 5 μm in diameter. Such structure with 5-μm spherulites was completely destroyed during annealing under a pressure of 400 MPa [see Fig. 14(b)], which was due to melting. New spherulites were formed during cooling with much smaller sizes.

Annealing under 480 MPa caused the degeneration of spherulites, as seen in Figure 14(c). That was because some of the lamellae got many folds thicker from 20 to 160 nm, whereas the crystallinity degree increased from 64 to only 85%. It meant that some of the crystals disappeared, whereas others dramatically increased their thicknesses. As follows from the WAXS studies, the thickening of existing lamellae took place. Because the orientation of existing lamellae was not lost, the spherulites preserved their initial

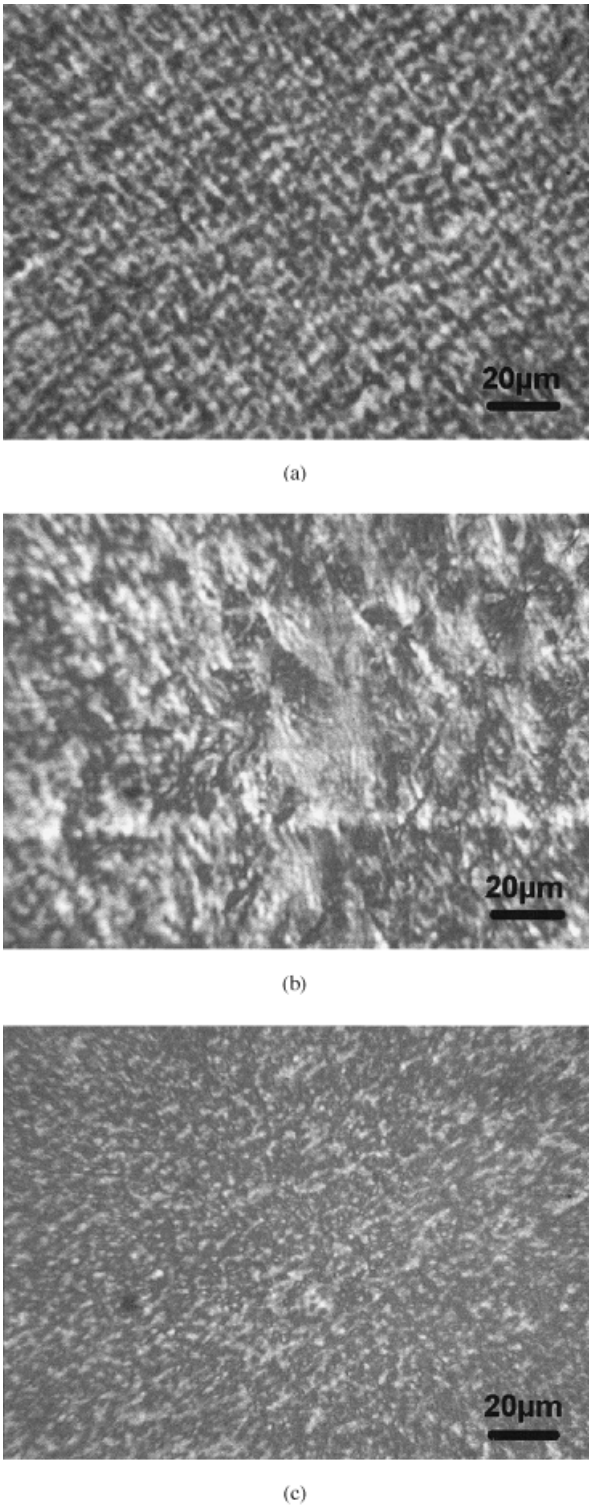

Figure 14 Light micrographs of microtomed 5 μm thick slices of high-density PE samples annealed under different conditions.

shape, but they now had a rough internal structure with very thick lamellae.

CONCLUSIONS

In conclusion, we can confirm that we developed an efficient way to obtain PE samples with a thickness value of crystals up to a very high value. The route to the pseudohexagonal phase through the orthorhombic phase, avoiding melting, leads to orthorhombic crystals with varying sizes. Parameters that influence the crystal size are the temperature, pressure, and time of annealing. Manipulation of these factors enabled us to produce crystals over a wide range of thicknesses. Annealing under high pressure caused an increase in the level of crystallinity.

Rearrangement of crystals, which takes place during annealing without passing through the molten state, occurred without loss of the original orientation of crystals. In this process, some crystals disappeared whereas some got thicker with no reorientation. Under such conditions, no new crystals with random orientation were formed. Oriented samples subjected to annealing in the pseudohexagonal region did not lose crystal orientation, whereas the crystals grew thicker, and the crystallinity degree increased to a very high level above 98%, as judged from the heat of melting of 288.6 J/g of the sample.

Noncrystalline regions shrunk as the crystal size and the crystallinity degree increased; however, no drastic change to their topology and structure was noticed, as followed from the unchanged position of the glass-transition temperature determined in the DMTA studies.

The authors wish to thank to Mrs. I. Kucinska for assistance in AFM investigations. They are very much indebted to Professor E. Duval from University Claude Bernard (Lyon-1, France) for the access to the Raman spectrometer and to Mr. M. Kozanecki for performing Raman experiments.

References

1. Argon, A. S. J Macromol Sci. Phys B 1973, 8, 573.
2. Bowden, P. B.; Raha, S. Philos Mag 1974, 29, 149.
3. Peterlin, A. J Mater Sci 1971, 6, 490.
4. Brooks, N. W. J.; Mukhtar, M. Polymer 2000, 41, 1475.
5. Sirotkin, R. O.; Brooks, N. M. Polymer 2001, 42, 3791.
6. Popli, R.; Mandelkern, L. J Polym Sci. Part B: Polym Phys 1987, 25, 441.
7. Wunderlich, B.; Arakawa, T. J Polym Sci Part A: Gen Pap 1964, 2, 3697.
8. Geil, P. H.; Aderson, F. R.; Wunderlich, B.; Arakawa, T. J Polym Sci Part A: Gen Pap 1964, 2, 3703.
9. Bassett, D. C.; Turner, B. Nat Phys Sci 1972, 240, 146.
10. Wunderlich, B.; Melillo, L. Macromol Chem 1968, 118, 250.
11. Prime, R. B.; Wunderlich, B. J Polym Sci Part A-2: Polym Phys 1969, 7, 2061.
12. Rees, D. V.; Bassett, D. C. J Polym Sci Part A-2: Polym Phys 1971, 9, 385.
13. Bassett, D. C.; Phillips, J. M. Polymer 1971, 12, 730.
14. Bassett, D. C.; Carder, D. R. Polymer 1973, 14, 387.
15. Bassett, D. C. Polymer 1976, 17, 460.
16. Bassett, D. C.; Turner, B. Philos Mag 1974, 29, 285.
17. Kowaleski, T.; Galeski, A. J Appl Polym Sci 1992, 44, 95.
18. Gruner, C. L.; Wunderlich, B.; Bopp, R. C. J Polym Sci Part A-2: Polym Phys 1969, 7, 2099.
19. Bassett, D. C.; Block, S.; Piermarini, G. J. J Appl Phys 1974, 45, 4146.
20. Yasuniwa, M.; Tsukbakihara, S.; Yamaguchi, M. J Polym Sci Part B: Polym Phys 1997, 35, 535.
21. Hatakeyama, T.; Hanetsuna, H.; Hashimoto, T. J Macromol Sci Phys B 1973, 7, 411.
22. Hoffman, J. D. Polymer 1983, 24, 3.
23. Hoffman, J. D. Polymer 1982, 23, 656.
24. Wunderlich, B.; Dole, M. J Polym Sci 1957, 24, 201.
25. Psarski, M.; Piorkowska, E.; Galeski, A. Macromolecules 2000, 33, 916.
26. Technical Note 211; Application Library; TA Instruments: New Castle, DE, 1997.
27. Olley, R. H.; Basset, D. C. Polymer 1982, 23, 1707.
28. Bartczak, Z.; Galeski, A.; Pluta, M. J Appl Polym Sci 2000, 76, 1746.
29. Schaufele, R. F.; Schimanouchi, T. J Chem Phys 1967, 47, 3605.
30. Fraser, G. V.; Hendra, P. J.; Willis, H. A.; Cudby, M. E. A. J Mater Sci 1974, 9, 1270.
31. Fraser, G. V.; Keller, A.; Pope, D. P. J Polym Sci Polym Lett Ed 1975, 13, 341.
32. Folkes, M. J.; Keller, A.; Stejny, J.; Goggin, P. L.; Fraser, G.; Hendra, P. J. Colloid Polym Sci 1975, 253, 354.
33. Dlugosz, J.; Fraser, G. V.; Grubb, D.; Keller, A.; Odell, J. A.; Goggin, P. L. Polymer 1976, 17, 471.
34. Rastogi, S.; Spoelstra, A. B.; Goossens, J. G. P.; Lemstra, P. J. Macromolecules 1997, 30, 7880.
35. Crist, B.; Rafner, M. A.; Brower, A. J.; Sabin, R. J. J Appl Phys 1979, 50, 6047.
36. Snyder, R. G.; Krause, S. J.; Schere, J. R. J Polym Sci Polym Phys ed 1978, 16, 1593.
37. Hoffman, J. D.; Ross, G. S.; Frolen, L.; Lauritzen, J. I., Jr. J Res Natl Bur Stand A, 1975, 79A, 671.
38. Zugenmaier, P.; Cantow H.-J. Kolloid Z Z Polym 1969, 230, 229.
39. Pakula, T.; Kryszewski, M.; Pluta, M. Eur Polym J 1977, 13, 141.
40. Kyu, T.; Suehiro, S.; Nomura, S.; Kawai, H. J Polym Sci Polym Phys Ed 1980, 18, 951.
41. Galeski, A.; Bartczak, Z.; Argon, A. S.; Cohen, R. E. Macromolecules 1992, 25, 5705.